Liquid Crystals
Publication details, including instructions for authors and subscription information:
http://www.informaworld.com/smpp/title~content=t713926090

Broad band dielectric relaxation spectroscopy of a chiral smectic B-crystal phase

F. Gouda[a]; S. T. Lagerwall[a]; K. Skarp[a]; B. Stebler[a]; F. Kremer[b]; S. U. Vallerien[b]
[a] Physics Department, Chalmers University of Technology, Göteborg, Sweden [b] Max-Planck-Institute für Polymerforschung, Mainz, Germany

To cite this Article Gouda, F. , Lagerwall, S. T. , Skarp, K. , Stebler, B. , Kremer, F. and Vallerien, S. U.(1994) 'Broad band dielectric relaxation spectroscopy of a chiral smectic B-crystal phase', Liquid Crystals, 17: 3, 367 — 379
To link to this Article: DOI: 10.1080/02678299408036577
URL: http://dx.doi.org/10.1080/02678299408036577

LIQUID CRYSTALS, 1994, VOL. 17, NO. 3, 367–379

Broad band dielectric relaxation spectroscopy of a chiral smectic B-crystal phase

by F. GOUDA*, S. T. LAGERWALL, K. SKARP and B. STEBLER
Physics Department, Chalmers University of Technology S-412 96, Göteborg, Sweden

F. KREMER and S. U. VALLERIEN
Max-Planck-Institute für Polymerforschung, Postfach 31 48. D-6500 Mainz, Germany

(*Received 8 October 1993; accepted 6 December 1993*)

By using dielectric relaxation spectroscopy it has been observed that while the molecular reorientation around the long axis in the smectic B-crystal phase is active, the rotation around the short axis is *frozen*. Thus we show that the molecular dynamics of the liquid crystal phase designated as smectic B-crystal is intermediate between that of crystals and that of conventional smectic phases (like smectic A, B, C etc.). The temperature dependence of the complex dielectric permittivity ε^* ($\varepsilon^* = \varepsilon' - j\varepsilon''$) has been studied in the frequency regime 10 Hz to 1 GHz on a binary mixture of a chiral epoxy compound and a non-chiral compound. The measurements were carried out on the isotropic phase (110–102°C), the narrow range cholesteric phase, the chiral smectic A phase (98–59°C), a chiral smectic B phase, so far classified as smectic B-crystal (59–33°C), and a crystal phase (below 33°C). The dielectric measurements were made for planar and homeotropic orientations. From the analysis of the dielectric absorption curves in the planar and homeotropic orientations, it is found that while the molecular reorientation around the long axis is characterized by a distribution of relaxation times, the rotation times, the rotation around the short axis is described by a single relaxation mechanism.

1. Introduction

Dielectric relaxation spectroscopy can be a powerful tool for studying molecular dynamics because it covers a broad frequency regime (10^{-3} to 10^{12} Hz); thus it has the ability to follow collective and non-collective molecular processes which exist in isotropic liquids, liquid crystals and other states of soft matter. While in isotropic liquids and the isotropic phase of liquid crystal materials, the molecular rotation is already relatively hindered and has a characteristic frequency in the microwave and high radio frequency regime, the rotation around the long and short axes of the molecules is frozen in the crystal phase. The situation in liquid crystalline phases, concerning the non-collective types of motion, is intermediate between the liquid and the crystal phases. The anisotropy of liquid crystal phases and the possibility of orienting the molecular director in directions parallel and perpendicular to a measuring electric field enables studies which may separate the molecular rotation around the short and long

* Author for correspondence.

0267–8292/94 $10·00

axis of the molecule. In this case, the dielectric spectrum of the parallel ($\varepsilon^*_\parallel$) and the perpendicular ($\varepsilon^*_\perp$) components of the complex dielectric permittivity have two distinct dielectric absorption and relaxation curves as traced, respectively, by the imaginary (ε'') and the real (ε') parts of the complex dielectric permittivity. The results of dielectric relaxation measurements made on the nematic phase [1–4], smectic A and C phases [5–9], and higher order smectic phases (B-crystal and hexatic, E, F, G, H, I) [10–13], are summarized at the end of a review article by Kresse [14], in which it is stated: 'From the experimental data in various LC phases it can be concluded that in all substances investigated until now, (1) a fast reorientation of the dipole moment around the molecular long axis and (2) a hindered reorientation around the short molecular axis exist. These two rotational possibilities should be typical for liquid crystals'.

Concerning the collective type of molecular reorientation observed in the chiral tilted and orthogonal phases, dielectric relaxation spectroscopy has been successfully applied [15–19] to characterize the soft mode and the Goldstone mode. The former is the collective tilt fluctuation of the molecular director observed in the chiral smectic A (A*) and chiral smectic C (C*) phases, and the latter is the collective phase fluctuation of the director in the C* phase.

The purpose of this paper is to present a dielectric study in the frequency regime 10 Hz to 1 GHz of the isotropic, cholesteric, smectic A* and smectic B*-crystal phase, showing the particular characteristics of the latter. From the measurements made for the perpendicular and the parallel components, it is found that molecular rotation around the long axis is active in all phases. However, while the rotation around the short molecular axis is only hindered in the smectic A* phase, it is completely frozen in the smectic B* crystal phase. Hence we have a first counter example to the statement cited above.

2. Experiment

The system studied was a binary mixture, with the components

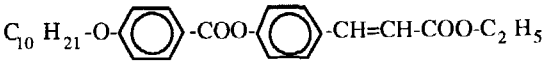

Non-chiral compound (Crystal 61·7 Smectic A 120·2 Isotropic)

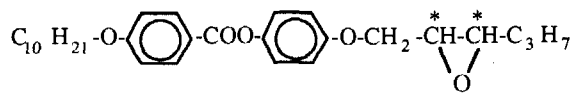

Chiral compound (Crystal 75 Smectic C*78 Cholesteric 95 Isotropic)

The transition temperatures (given in degrees Celsius) of the mixture have been determined by differential scanning calorimetry (DSC) and optical microscopy to be

Crystal–30–B*–60–A*–98–N*–102–Isotropic.

The nature of the smectic A*–smectic B*-crystal transition has been characterized by DSC. From different scans made on both cooling and heating runs, a clear hysteresis in the A*–B* transition temperature has been found, thus indicating that the smectic A*–B*-crystal transition is first order. The hysteresis in the transition temperature depends on the cooling and heating rates; for instance at 2°C min^{-1}, the hysteresis ΔT was found to be 0·79°C.

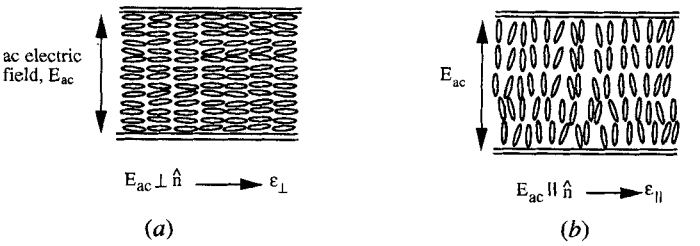

Figure 1. The two measurement geometries in the smectic A* and B* phases. (*a*) Planar orientation: the smectic layers are aligned perpendicular to the electrode (or glass) plates. This measurement geometry permits measurements of the perpendicular component of the complex dielectric permittivity $\varepsilon^*_\perp$. (*b*)Homeotropic orientation: the smectic layers are aligned parallel to the glass plates. This measurement geometry permits measurements of the parallel component of the complex dielectric permittivity $\varepsilon^*_\parallel$.

The existence of the smectic B*-crystal phase has been confirmed by means of X-ray measurements. From the Guiner patterns of a non-directed sample, the smectic B*-crystal phase has been clearly distinguished from the A* and the crystal phase observed at higher and lower temperatures, respectively.

The complex dielectric permittivity (ε^*, $\varepsilon^* = \varepsilon' - j\varepsilon''$) has been measured in the frequency regime 10 Hz to 1 GHz using the Hewlett Packard 4192 LF impedance analyser (5 Hz–10 MHz) and 4191A RF impedance analyser (1–1000 MHz). The experiments were performed in two measurement geometries to determine the principal components $\varepsilon^*_\parallel$ and $\varepsilon^*_\perp$ of the dielectric tensor. For the $\varepsilon^*_\perp$ measurements in the low frequency regime, 10 Hz–13 MHz, the cell consisted of two glass plates coated with conducting layers made of indium tin oxide (ITO) separated by a mylar spacer of 12 μm. The active area of our cell was 30 mm^2. The glass surfaces were not treated with any surfactant after cleaning with acetone. The sample was cooled from the isotropic phase to the cholesteric and to the smectic A* phase in the presence of an A.C. electric field of 10 V/50 μm. This gives a planar orientation, i.e. with the smectic layers standing perpendicular to the glass plate, as checked by optical microscopy. The measuring electric field of 1 V/50 μm, as shown in figure 1 (a), was applied in a direction perpendicular to the director; hence we measured the perpendicular component of the dielectric tensor. In the high frequency regime, although microscopic observation was not possible because of the cell construction [20], nevertheless, this measurement geometry was identified from the dielectric absorption peak observed in the range of 100 MHz, as will be discussed latter. The high frequency measurements were made on a sample of 50 μm thickness. The $\varepsilon^*_\parallel$ measurements were only made in the range 10 Hz to 10 MHz. The cell was similar to that used for planar orientation. However, the glass plates, in this case, were coated with surfactant (Quilon C) to get a homeotropic orientation. In this geometry (see figure 1 (*b*)), the measuring electric field is applied in a direction parallel to the director.

In the frequency range 10 Hz to 10 MHz, the measured dielectric absorption ε'', contains, besides the absorption peak due to molecular rotation, additional contributions at low and high frequencies which have to be corrected for as shown in figure 2. At low frequencies, the measured ε'' has a conductivity contribution due to the non-bound charge carriers (this is also called DC conductivity): the measured ε'' increases with decreasing frequency, and in the worst cases may obscure relaxation peaks due to dipolar rotation. At high frequencies, because of the ITO conducting layer

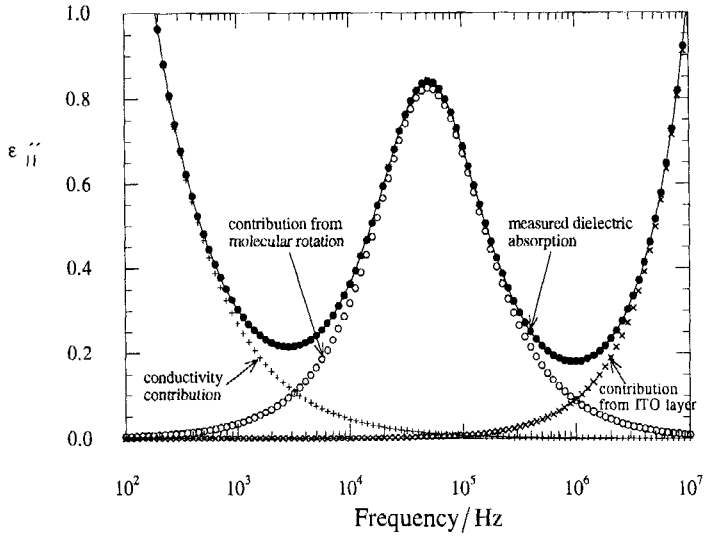

Figure 2. Illustrative example of the frequency dependence of the measured dielectric absorption $\varepsilon''_{\parallel}$ in the homeotropic orientation. Besides the contribution from dipolar reorientation (open circles), there is a low frequency background from freely moving charges (+). At high frequency the background is due to the ITO conducting layer (×). The solid line represents the fitting of the experimental data to equation (1).

of about 20 Ω/□ resistance, the measured ε'' increases at frequencies ≥ 1 MHz. In order to extract the correct values of the dielectric contribution of a certain molecular process from this background at both low and high frequencies, the measured dielectric absorption has been fitted to an equation of the form [18]

$$\varepsilon'' = \frac{\sigma}{2\pi\varepsilon_0}\left(\frac{1}{f^n}\right) + \mathrm{Im}\left(\varepsilon_\infty + \frac{\Delta\varepsilon}{1+\left(j\frac{f}{f_R}\right)^{1-\alpha}}\right) + a(R,C)f^m. \tag{1}$$

The first term represents the DC conductivity contribution in which σ is the specific conductivity of the sample ($\mathrm{ohm}^{-1}\,\mathrm{cm}^{-1}$), f is the frequency of the measuring AC electric field and ε_0 is the vacuum permittivity. Both σ and n are fitting parameters. The second term is the imaginary part in the Cole–Cole equation [21], where $\Delta\varepsilon$ is the dielectric strength which is the difference between the dielectric permittivity measured at low ε_S and high ε_∞ frequencies, f_R is the relaxation frequency, and α is a symmetric distribution parameter. The third term represents the high frequency contribution, where $a(R, C)$ is a fitting parameter which depends on the time constant of the cell, i.e. the resistance R of the ITO layer and the cell capacitance C. The fitting parameter n in most cases tends to be near one.

3. Results and discussion

3.1. *The static dielectric permittivity*

The temperature dependence of the parallel and perpendicular components of the static dielectric permittivity measured in different phases is shown in figure 3. In the isotropic phase, the real part of the dielectric permittivity ε is about 4·75 at 110°C and increases with decreasing temperature. In the cholesteric phase, N*, within our measurement accuracy, the measured ε behaves in a similar way to that in the isotropic

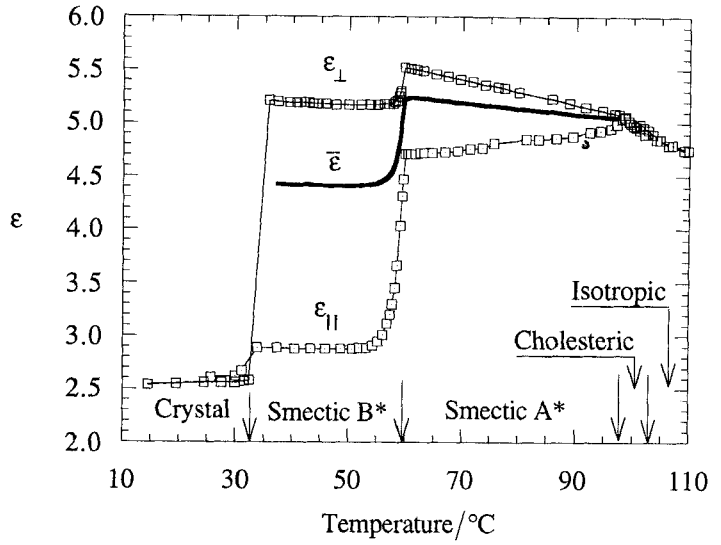

Figure 3 Temperature dependence of the static dielectric permittivity measured in different phases.

phase; we were not able to resolve a remarkable difference between the values of $\varepsilon_\parallel$ and $\varepsilon_\perp$ in this phase. However, at the N* to smectic A* transition, the values clearly split. While the perpendicular component $\varepsilon_\perp$ increases with decreasing temperature, the parallel component $\varepsilon_\parallel$ behaves in an opposite manner. The decrease in $\varepsilon_\parallel$ is usually attributed to an antiparallel correlation between the dipole moments along the long axes of the molecules [22]. At the transition from the smectic A* phase to the smectic B*-crystal phase, a sharp drop in $\varepsilon_\parallel$ from 4·7 to 2·9 is observed. A further drop in both $\varepsilon_\parallel$ and $\varepsilon_\perp$ is observed at the transition to the crystal phase; $\varepsilon_\perp$ decreases from 5·20 to 2·55, and $\varepsilon_\parallel$ decreases from 2·90 to 2·60. In the smectic A* and B* phases, $\varepsilon_\perp$ is larger than $\varepsilon_\parallel$, and this means that the dielectric anisotropy $\varepsilon_a = \varepsilon_\parallel - \varepsilon_\perp$ is negative and increases with decreasing temperature. The largest value of ε_a in the smectic A* phase, as can be seen from figure 3, is about $-0{\cdot}8$. In the B* phase, ε_a equals $-2{\cdot}3$. Another quantity of importance is the average value of the dielectric permittivity $\bar{\varepsilon} = (\varepsilon_\parallel + 2\varepsilon_\perp)/3$. In the case of a strongly polar compound, $\bar{\varepsilon}$ shows a drop while cooling from the isotropic to the nematic phase [23]. In our case, the dielectric permittivity in the isotropic phase increases with decreasing temperature, and in the smectic A* phase, $\bar{\varepsilon}$ does not show any appreciable drop; however, the slope $d\bar{\varepsilon}/dT$ is smaller relative to that in the isotropic phase. In the smectic B*-crystal phase, we observe that $\bar{\varepsilon}$ is considerably less than that of the smectic A* phase; it decreases by 20 per cent. This indicates that the dipolar reorientation in the smectic B*-crystal phase is strongly restricted compared with the situation in the smectic A* phase.

In the crystal phase, the permittivity values ($\varepsilon_\perp = 2{\cdot}6$ and $\varepsilon_\parallel = 2{\cdot}9$) are slightly larger than the square of the refractive index n. Though we did not measure the value of n for this system, it is known from the literature that most liquid crystal materials have values of n^2 which are less than 2·9 and 2·6. This difference may be attributed to an intramolecular rotation which is still active in the crystal phase.

It is worth pointing out that in the smectic A* phase, besides the high frequency molecular contribution to the permittivity, $\varepsilon_\perp$ has a contribution from the soft mode

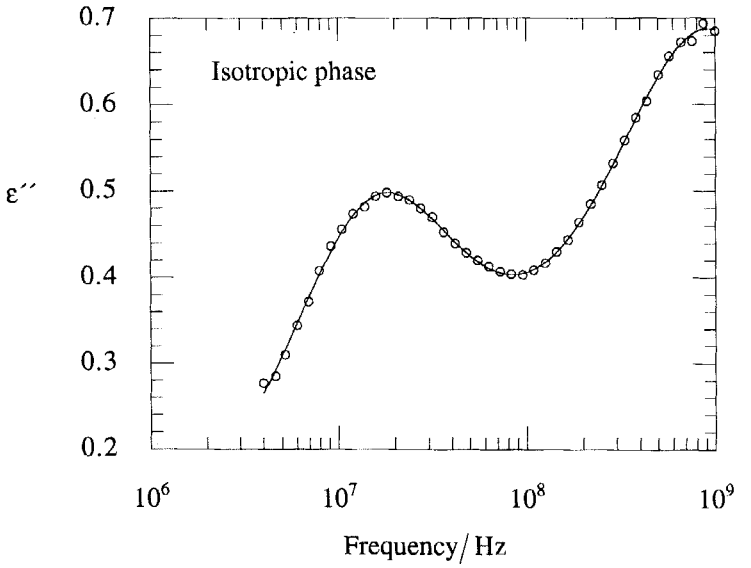

Figure 4 Frequency dependence of the dielectric absorption measured in the isotropic phase. The solid line represents the fitting of the experimental data to equation (2).

(tilt fluctuation). The soft mode contribution to $\varepsilon_\perp$ increases linearly with decreasing temperature, from 5·0 at 98°C to 5·5 at 60°C, and does not show any divergence at the smectic A*–B* transition T_C, a point which has been discussed, for this system in detail elsewhere [24].

3.2. *The dynamic dielectric permittivity*

In the isotropic phase, the dielectric spectrum exhibits two absorption peaks as shown in figure 4. In order to characterize these two relaxations, the experimental points have been fitted to the Cole–Cole equation [21] for the case of superposition of two absorptions

$$\varepsilon'' = \mathrm{Im}\left(\varepsilon_\infty + (\varepsilon_S - \varepsilon_\infty)\left(\frac{g_1}{1+\left(j\frac{f}{f_{R1}}\right)^{1-\alpha_1}} + \frac{g_2}{1+\left(j\frac{f}{f_{R2}}\right)^{1-\alpha_2}}\right)\right), \tag{2}$$

where g_1 and g_2 are weighting factors connected by $g_1 + g_2 = 1$, and α_1 and α_2 are the distribution parameters of the first and second absorption peaks. In the case of a single relaxation time mechanism (Debye relaxation) $\alpha = 0$. From the fitting, we found the dielectric strength $\Delta\varepsilon$, $(\varepsilon_S - \varepsilon_\infty) = 2{\cdot}20$, $g_1 = 0{\cdot}39$, $\alpha_1 = 0{\cdot}13$, and $\alpha_2 = 0{\cdot}27$. The relaxation frequencies of the low and high frequency mechanisms are 15·7 MHz and 986·3 MHz, respectively. From these values, we conclude that the low and high frequency absorptions are connected with the molecular rotations around the short and long axes of molecule. In the vicinity of the N*–A* transition, these two absorptions could still be traced. However, at the onset of the A* phase, while the amplitude of high frequency absorption was found to increase with decreasing temperature, the amplitude of the low frequency absorption strongly decreased and, at one degree below the N*–A* transition, the peak disappeared completely and only the high frequency absorption could be observed in the spectrum. This indicates that, within the accuracy of our

measurements, the measurement geometry obtained in the high frequency cell is a planar orientation. At this point, it is worth noting that the dielectric spectrum of chiral smectics contains an additional absorption peak due to the collective tilt fluctuations (the soft mode) [15–19]. The characteristic frequency of the soft mode exhibits a strong temperature dependence, usually observed in the kHz region of the dielectric spectrum. However, in our case, this peak could not be observed, probably because the dipole moment connected with this process is very weak. This has been confirmed from the electrically induced tilt angle [24] due to the electroclinic effect, which was found to be of the order of 0·1°, a value which is less than that measured for most compounds by one or two orders of magnitude.

The experimental values of $\varepsilon''_\perp$ versus frequency have been fitted to the Havriliak–Negami relation [25]

$$\varepsilon''_\perp = \mathrm{Im}\left\{\varepsilon_\infty + \frac{\varepsilon_S - \varepsilon_\infty}{\left[1 + \left(j\frac{f}{f_{R\perp}}\right)^{1-\alpha_\perp}\right]^\beta}\right\}, \tag{3}$$

where β is the asymmetric distribution parameter. From the fitting, the distribution parameters are $\alpha = 0{\cdot}17$ and $\beta = 0{\cdot}79$, and the relaxation frequency is found to be $f_{R\perp} = 330\,\mathrm{MHz}$ (at 80·15°C). The molecular aspect of this relaxation corresponds to rotation around the long axis of the molecules. The relaxation frequency decreases slightly with decreasing temperature. In the smectic B*-crystal phase, this molecular motion is active, but slower than that found in the smectic A* phase. From the fitting results of the data shown in figure 5 (*a*), the relaxation $f_{R\perp}$ in the smectic B*-crystal phase (at 55·18°C) equals 95·0 MHz. Figure 5 (*b*) shows the frequency dependence of $\varepsilon''_\perp$ in the different phases. While the absorption maximum, $\varepsilon''_\perp$ (max), in the smectic A* phase increases with decreasing temperature (from right side to left side in figure 5 (*b*)), it decreases in the smectic B*-crystal phase. This may give an indication that the three-dimensional order in the smectic B*-crystal phase influences the molecular rotation in such a way that it becomes strongly hindered, as compared with that in the smectic A* phase, where one may think of an overall continuous reorientation through multiple collisions with the surroundings. However, in the presence of such high order, we may have a symmetric potential, but with multiple minima. At the onset of crystallization, $\varepsilon''_\perp$(max) decreases sharply, and on further cooling, disappears completely from the spectrum, thus indicating that the overall rotation of the molecules as a whole around the long axes is frozen.

The dielectric absorption measurements in the parallel orientation $\varepsilon''_\parallel$ have been made in the range 10^1 to 10^7 Hz. No significant results were found below 10^3 Hz; therefore, the results are mainly presented for the frequency regime 10^3 to 10^6 Hz. Figure 6 (*a*) shows the frequency dependence of $\varepsilon''_\parallel$ in the smectic A phase at 86·52°C. The data have been fitted to equation (1). The distribution parameter α equals 0·02; thus the relaxation mechanism in this measuring geometry, which corresponds to molecular rotation around the short axis, is described by a single relaxation (Debye relaxation). The relaxation frequency at this temperature equals 94·3 kHz. Over the whole range of the smectic A phase, the relaxation frequency decreases from 1 MHz at 96·00°C to 30 kHz at 60°C. At the first order smectic A* to smectic B*-crystal phase transition temperature T_C, the absorption maximum shows a pronounced decrease. In order to avoid supercooling, the temperature was very slowly decreased ($\approx 0{\cdot}01\,^\circ\mathrm{C\,min^{-1}}$) at T_C and below. Within a temperature range of 4°C, the absorption maximum (indicated

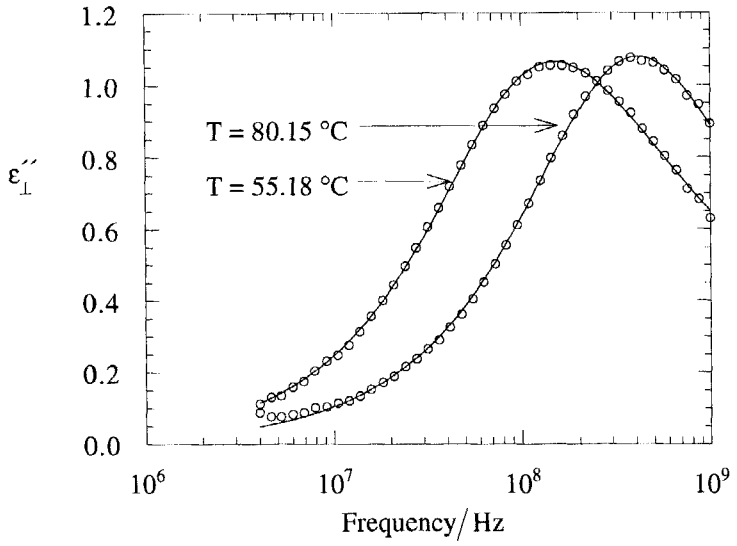

(*a*)

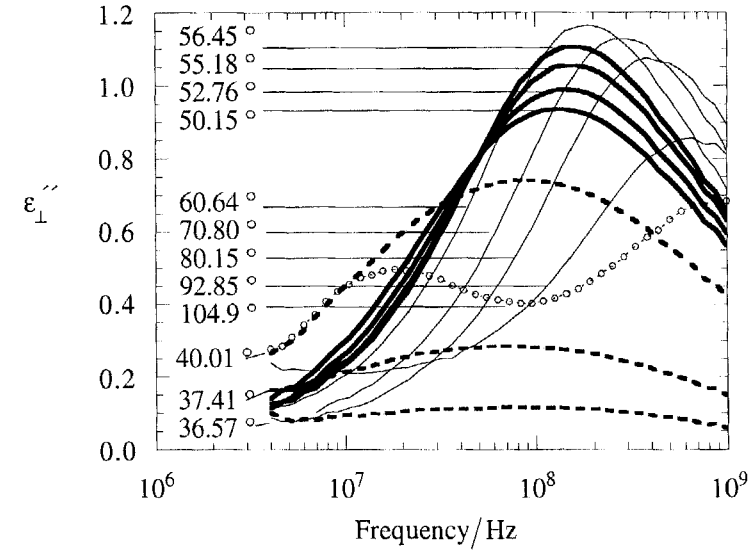

(*b*)

Figure 5. (*a*) Frequency dependence of the perpendicular component of the dielectric absorption measured in the smectic A* phase (at 80·15°C) and in the smectic B*-crystal phase (at 55·18°C). The solid lines represent the fitting of the experimental data to equation (3). (*b*) Frequency dependence of the dielectric absorption measured in the isotropic phase, at different temperatures in the isotropic (circles), smectic A* (thin solid lines), and B*-crystal (thick solid lines) phases and in the crystal phase (dashed lines).

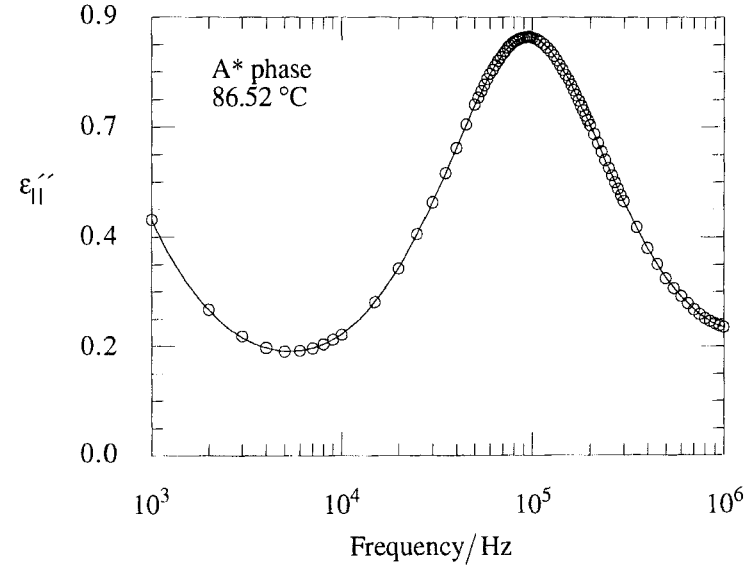

(*a*)

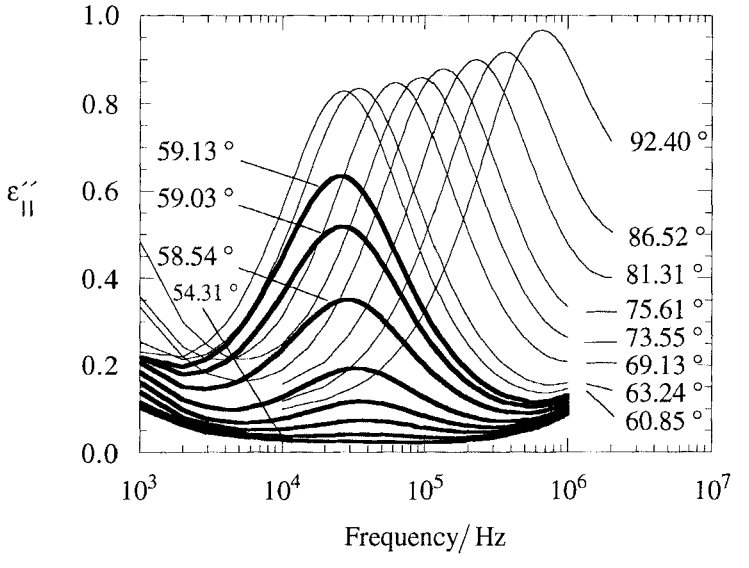

(*b*)

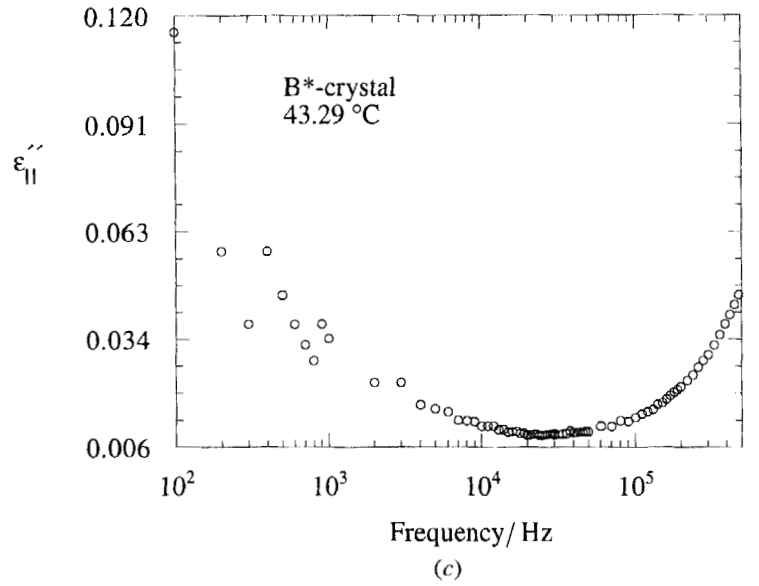

Figure 6. (*a*) Frequency dependence of the parallel component of the dielectric absorption measured in the smectic A* phase (at 86·52°C). The solid line represents the fitting of the experimental data to equation (1). (*b*) Frequency dependence of the dielectric absorption measured in the isotropic phase and at different temperatures in the smectic A* phase (thin lines) and B*-crystal phase (thick lines). (*c*) Frequency dependence of the parallel component of the dielectric absorption measured in the smectic B*-crystal phase (at 43·29°C).

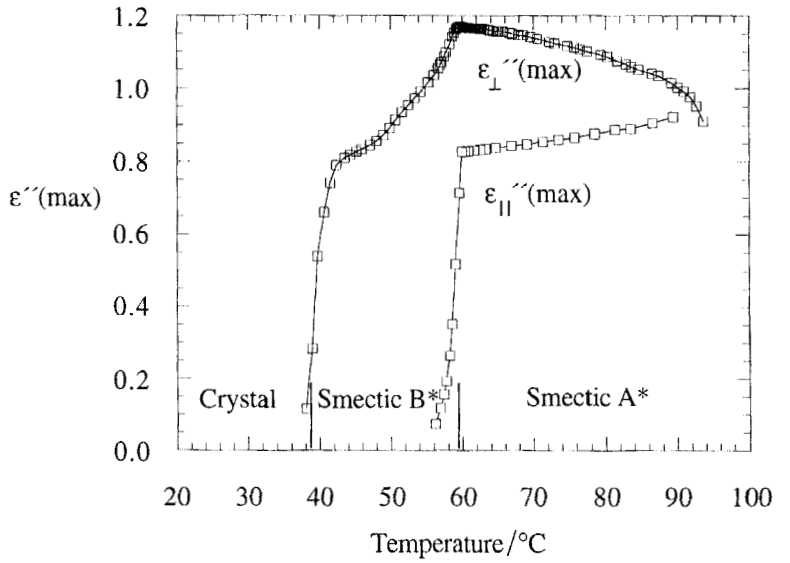

Figure 7. Temperature dependence of the dielectric absorption maximum in the smectic A* and B*-crystal phases. Notice how the molecular rotation around the short axis ($\varepsilon''_{\parallel}$) freezes out at the transition smectic A*–smectic B*-crystal and how the rotation around the long axis ($\varepsilon''_{\perp}$) does the same at the transition smectic B*-crystal–crystal.

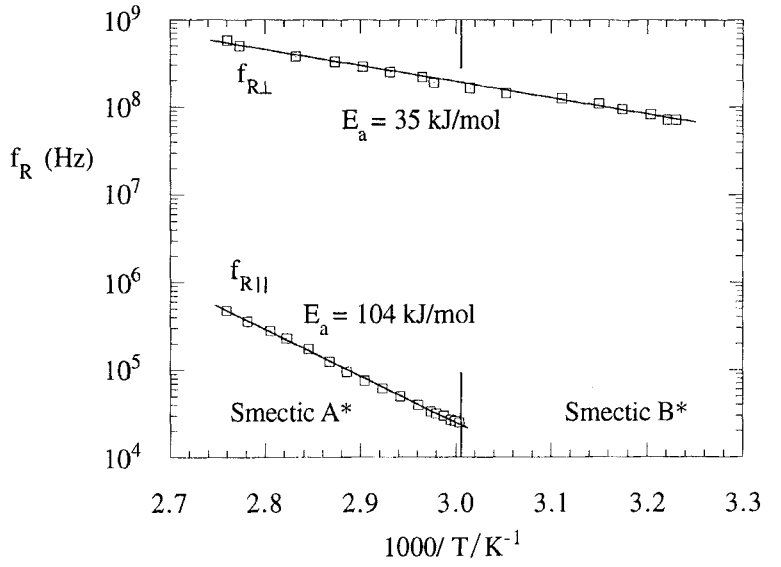

Figure 8. Arrhenius plot of relaxation frequency for the molecular rotation around the long and short axes.

by thick lines in figure 6(*b*) is centred around 30 kHz and its amplitude strongly decreases with temperature, until it disappears completely from the spectrum. Figure 6(*c*) shows, on an enlarged scale, the spectrum of $\varepsilon''_{\parallel}$ at a lower temperature (43·29°C). This figure does not reveal any absorption-like behaviour; it contains, as explained in detail in the experimental section, the background at low and high frequencies. In order to sort out the possibility that this peak is shifted to much lower frequencies, similar dielectric absorption measurements have been made using a lock-in amplifier to get more accurate values. These measurements were made in the frequency range 1 Hz to 20 kHz and did not give any indication of any absorption peak in the smectic B*-crystal phase. We think that the absorption peaks observed within 4°C below T_C (see figure 6(*b*)) are just a result of the coexistence of the smectic A* and B* phases. This temperature interval represents a two-phase region in which the remaining part of the smectic A* phase is responsible for the absorption peaks in the smectic B*-crystal phase. From these measurements made in the homeotropic orientation in the smectic B*-crystal phase, it is confirmed that the molecular rotation around the short molecular axis in the crystal smectic B* phase is frozen. In contrast with earlier [10–12] and recent [13] reports concerning this molecular mechanism, we think that this example shows that this molecular rotation is locked in the smectic B*-crystal phase. In this context, it is interesting to point out that the disappearance of the dielectric absorption peak which corresponds to the molecular rotation around the short axis of molecule in the smectic B*-crystal phase is similar to that for molecular rotation around the long molecular axis in the crystal phase. Figure 7 shows the temperature dependence of ε''(max) in the planar and homeotropic orientations in the smectic A*, B* and crystal phases. The interesting point in this figure is the similarity between the sharp drops in $\varepsilon''_{\parallel}$(max) and $\varepsilon''_{\perp}$(max) at the smectic A*–B* transition and the smectic B*-crystal–crystal transition, respectively.

The relaxation frequency calculated for the molecular rotation around the long axis in the smectic A* and B* phases, and the molecular rotation around the short axis in

the smectic A* phase have been plotted against $1/T$ as shown in figure 8 (Arrhenius plot). The activation energy $E_{a(\parallel)}$ for the molecular rotation around the short axis, as one would expect, is larger than $E_{a(\perp)}$ for the rotation around the long axis. In our case,

$$E_{a(\parallel)}(\text{A* phase}) \approx 3E_{a(\perp)}(\text{A*, B* phases}).$$

As can be seen from figure 8, values of $f_{r\perp}$ in the smectic A* and B* phases lie on the same line, showing no jump at T_C. The disappearance of the dielectric absorption $\varepsilon''_{\parallel}$ in the smectic B*-crystal, which is interpreted as a freezing of the molecular motion, thus implies an inhibitive value of the activation energy.

4. Conclusions

We have presented broad band (10 Hz to 1 GHz) dielectric relaxation spectroscopy measurements of the two principal axes of complex dielectric permittivity in the smectic A*, smectic B*-crystal, isotropic and crystal phases of a binary mixture. While in the isotropic phase, the molecular rotations around the long and short axes are active, these main molecular rotations in the crystal phase, as seen from the finite difference between the permittivity and the square of the refractive index. The molecular dynamics of the liquid crystalline state manifests the molecular motion of the isotropic liquid and the crystal state. While the molecular rotation around the long axis in the smectic A* and smectic B*-crystal phase is active, with an activation energy of about 35 kJ mol^{-1}, the molecular rotation around the short axis in the smectic B*-crystal phase is completely frozen. In the smectic A* phase, this rotation is active with an activation energy equal to 104 kJ mol^{-1}. From the analysis of the dielectric absorption curves in the isotropic, smectic A* and smectic B*-crystal phases, we find a relatively large value of the symmetric distribution parameter connected with the dipolar rotation around the long axis. We may conclude from this result that different processes are involved: for instance [26], the rotation of the molecule as a whole, independent reorientation of the alkyl group around the single bond to the neighbouring benzene ring and small angle reorientation of the permanent dipole moment around the director. The result concerning the molecular dynamics in the chiral smectic B*-crystal phase, adds a new category of liquid crystal phase which has a frozen molecular rotation around the short axis, but activated rotation around the long axis.

The authors are grateful to Dr S. Diele (Halle, Germany) for carrying out the X-ray studies.

References

[1] Meier, W., and Meier, G., 1961, *Z. Naturf.* (*a*), **16,** 1200.
[2] Meier, G., and Saupe, A., 1966, *Molec. Crystals*, **1,** 515.
[3] Buka, A., Owen, P. G., and Price, A. H., 1979, *Molec. Crystals liq. Crystals*, **51,** 273.
[4] Parneix, J. P., and Chapoton, A., 1981, *Molec. Crystals liq. Crystals.*, **78,** 115.
[5] Druon, C., and Wacrenier, J. M., 1977, *J. Phys., Paris*, **38,** 47.
[6] Kresse, H., Wiegeleben, A., and Demus, D., 1980, *Crystal. Res. Technol.*, **15,** 341.
[7] Bata, L., and Buka, A., 1981, *Molec. Crystals liq. Crystals*, **15,** 341.
[8] Buka, A., and Bata, L., 1980, *Adv. Liq. Cryst. Res. Appl., Proc. Liq. Cryst. Conf.* (Pergamon Press), p. 261.
[9] Druon, C., and Wacrenier, J. M., 1984, *Molec. Crystals liq. Crystals*, **108,** 291.
[10] Buka, A., Bata, L., Pinter, K., and Szabom, J., 1982, *Molec. Crystals liq. Crystals Lett.*, **72,** 285.
[11] Gajewska, B., Kressf, H., and Weissflog, W., 1982, *Crystal. Res. Technol.*, **17,** 897.
[12] Kresse, H., and Buka, A., 1982, *Crystal. Res. Technol.*, **17,** 1123.

[13] NAGABHUSHAN, C., NAIR, G., RATNA, B. R., SHASHIDAR, R., and GOODBY, J. W., 1988, *Liq. Crystals*, **3,** 175.
[14] KRESSE, H., 1983, *Adv. Liq. Crystals*, **6,** 109.
[15] OSTROVSKII, B. I., RABINOVICH, A. Z., SONIN, A. S., and STRUKOV, E. A., 1978, *Soviet Phys. JETP*, **47,** 912.
[16] LEVSTIK, A., CARLSSON, T., FILIPIC, C., LEVSTIK, I., and ZEKS, B., 1987, *Phys. Rev.* A, **35,** 3527.
[17] PAVEL, J., GLOGAROVA, M., and BAWA, S., 1987, *Ferroelectrics*, **76,** 221.
[18] GOUDA, F., SKARP, K., and LAGERWALL, S. T., 1991, *Ferroelectrics*, **113,** 165.
[19] KREMER, F., and VALLERIEN, S. U., 1990, *Phys. Rev.* A, **42,** 3667.
[20] KREMER, F., BOESE, D., MEIER, G., and FISCHER, E. W., 1989, *Prog. Coll. Polym. Sci.*, **80,** 129.
[21] COLE, K. S., and COLE, R. H., 1941, *J. chem. Phys.*, **9,** 341.
[22] DE JEU, W. H., GOOSSENS, W. J. A., and BORDERWIJK, P., 1974, *J. chem. Phys.*, **61,** 1985.
[23] BRADSHAW, M. J., and RAYNES, E. P., 1983, *Molec. Crystals liq. Crystals*, **91,** 145.
[24] GOUDA, F., CARLSON, T., FLATICHLER, K., KOMITOV, L., LAGERWALL, S. T., SKARP, K., and STEBLER, B., 1992, *Phys. Rev.* A, **45,** 5362.
[25] HAVRIALIAK, S., and NEGAMI, S., 1966, *Polymer*, C14, **8,** 99.
[26] KRESSE, H., and MOSCICKI, J. K., 1980, *Adv. Liq. Cryst. Res. Appl., Proc. Liq. Cryst. Conf.* (Pergamon Press), p. 287.